Available online at www.sciencedirect.com
SCIENCE DIRECT®
PERGAMON
Physics and Chemistry of the Earth 28 (2003) 499–509
PHYSICS and CHEMISTRY of the EARTH
www.elsevier.com/locate/pce

Influence of temperature on thermal conductivity, thermal capacity and thermal diffusivity for different types of rock

Hans-Dieter Vosteen [a,*], Rüdiger Schellschmidt [b]

[a] Applied Geophysics, Aachen University (RWTH), Lochnerstr. 4-20, D-52056 Aachen, Germany
[b] Leibniz Institute for Applied Geosciences (GGA), Stilleweg 2, 30655 Hannover, Germany

Received 10 August 2002; received in revised form 20 November 2002; accepted 4 April 2003

Abstract

Thermal modeling down to great depth, e.g. down to the Mohorovicic discontinuity, requires representative values of thermal conductivity and thermal capacity at an appropriate depth. Often there is a lack of data, especially concerning temperature and pressure dependence of thermal conductivity and thermal capacity, due to missing or questionable data from boreholes. Studies of the temperature and pressure dependence of thermal conductivity and thermal capacity showed that temperature is dominating. Thus measurements on a set of magmatic, metamorphic and sedimentary rocks sampled from different depth levels of the Eastern Alpine crust were used to obtain an estimate of the temperature dependence of both properties—at least for the area of investigation—and to give a review of the temperature dependence of thermal conductivity (λ), thermal capacity ($\rho \times c_p$) and thermal diffusivity (κ) for different types of rock.

The temperature dependence of thermal conductivity for crystalline (magmatitic and metamorphic) rocks is different to that of sedimentary rocks. Using the approach that the thermal resistivity ($1/\lambda$) is a linear function of temperature whose slope increases with $\lambda(0)$, the conductivity at a temperature of 0 °C, two general equations were determined. The equation for crystalline rocks was verified in the temperature range of 0–500 °C and the equation for sedimentary rocks was tested in the temperature range from 0 to 300 °C. A general equation for the temperature dependence of λ for Eastern Alpine rocks can thus be formulated:

$$\lambda(T) = \frac{\lambda(0)}{0.99 + T(a - b/\lambda(0))}$$

with empirical constants and corresponding uncertainties $a = 0.0030 \pm 0.0015$ and $b = 0.0042 \pm 0.0006$ for crystalline rocks. The constants for corresponding sedimentary rocks are $a = 0.0034 \pm 0.0006$ and $b = 0.0039 \pm 0.0014$. λ is given in $\mathrm{W\,m^{-1}\,K^{-1}}$, T in °C.

At ambient conditions thermal diffusivity (κ) and thermal conductivity (λ) for Eastern Alpine crystalline rocks show the relationship:

$$\kappa = 0.45 \times \lambda.$$

Keywords: Geothermics; Rock physics; Thermal conductivity; Temperature dependence; Thermal capacity; Thermal diffusivity

1. Introduction

As a part of the European multidisciplinary TRANSALP campaign to investigate the Eastern Alpine orogenic processes (TRANSALP Working Group, 2002), a project was set up to (1) obtain a complete data set of the thermophysical properties of the main rock units of the Eastern Alpine crust and (2) model the steady state conductive heat transport. Due to the lack of rock samples from deep boreholes, we took advantage of the complex tectonics, which yield representative outcrops of rocks from nearly all depth levels of the Eastern Alpine crust. According to the resolution of the finite element grid the main sampling criterion for each rock unit was an estimated minimum thickness of 1 km in the cross section along our profile. We performed laboratory measurements of thermal conductivity, specific heat capacity, density, and porosity on this collection of newly gained rock samples from 26 different substantial

* Corresponding author. Tel.: +49-241-80-96773; fax: +49-241-80-92132.
E-mail address: h.vosteen@geophysik.rwth-aachen.de (H.-D. Vosteen).

1474-7065/03/$ - see front matter © 2003 Elsevier Science Ltd. All rights reserved.
doi:10.1016/S1474-7065(03)00069-X

rock units of the Eastern Alps. We also determined the temperature dependence of thermal conductivity $\lambda(T)$ and specific heat capacity $c_p(T)$. Concerning the temperature dependence of thermal conductivity, a coupled effect of mineralogical composition and temperature can be assumed whenever the thermal resistivity $(1/\lambda)$ is a linear function of temperature whose slope increases with $\lambda(0)$, the conductivity at a temperature of 0 °C.

A general equation for $\lambda(T)$ was set up by Sass et al. (1992) which is based on the coupled effect of composition and temperature on thermal conductivity. In order to determine this relation for crystalline rocks, Sass et al. (1992) used thermal conductivity data from six different granites measured by Birch and Clark (1940) up to a maximum temperature of 200 °C. The equation was further successfully verified for an independent set of different magmatic and metamorphic rocks from the Valles Caldera (Sibbitt et al., 1979) for temperatures ranging from 25 to 250 °C.

Above a certain temperature, this equation leads to large deviations from the measured values. This results from the heat transfer by radiation, which becomes important for single crystals at temperatures of approximately 200 °C and for polycrystals at approximately 600 °C (Clauser, 1988; Clauser and Huenges, 1995).

In this study we attempted to (a) check the adaptability of the existing coefficients of Sass et al. (1992) for our newly gained rock samples and (b) determine new coefficients to extend the temperature range for the equation of Sass et al. (1992) for both crystalline and sedimentary rocks of the Eastern Alps.

Different approaches to calculate $\lambda(T)$ were developed by Zoth and Hänel (1988) and Seipold (1998, 2001) and will be discussed in detail. Pribnow et al. (2000) studied $\lambda(T)$ for water saturated marine sedimentary rocks for temperatures from 0 to 60 °C. In this temperature interval for marine sedimentary rocks with a low thermal conductivity at ambient conditions (λ_{rt}) they found that thermal conductivity increases with temperature. For rock samples with intermediate values of λ_{rt} thermal conductivity remains unchanged with temperature and decreases with temperature for rocks with high λ_{rt}. Pribnow et al. (2000) maintain that this behavior is due to a positive temperature coefficient for seawater (λ increases with T) and a negative coefficient for the rock matrix (λ decreases with T). As we studied the temperature dependence of thermal conductivity for dry rock samples only, and at much higher temperatures, our results are not directly comparable to those of Pribnow et al. (2000) but rather complement their study in respect to the larger temperature range.

Thermal diffusivity κ is the ratio of thermal conductivity λ and thermal capacity $\rho \times c_p$. Thus our data set also permits a discussion on the variation of thermal diffusivity with temperature for different rocks of the Eastern Alps.

2. Measured properties

We collected a total of 118 rock samples for thermal property measurements in a campaign at 26 locations along the TRANSALP-profile (Fig. 1) during the summer of 1999. On these specimens bulk density ρ_b, rock density ρ_r, heat production rate, specific heat capacity c_p and thermal conductivity λ of dry and of water saturated rock were determined in the laboratory. Additional information concerning measurement techniques is summarized in the Appendix A. For further details on the sampling strategy and on measurements of the heat production rate refer to the companion paper by Vosteen et al. (this issue).

2.1. Rock density and porosity

Both rock density and bulk density were determined of all rock samples. Rock density ρ_r is defined as the ratio of the dry mass M of a rock and the pure rock volume V_r excluding the volume of any cavities. By contrast, bulk density ρ_b is defined as the ratio of the dry rock mass M and the bulk rock volume V_b including the volume of all cavities in the rock.

Rock porosity ϕ can be determined from rock and bulk density according to:

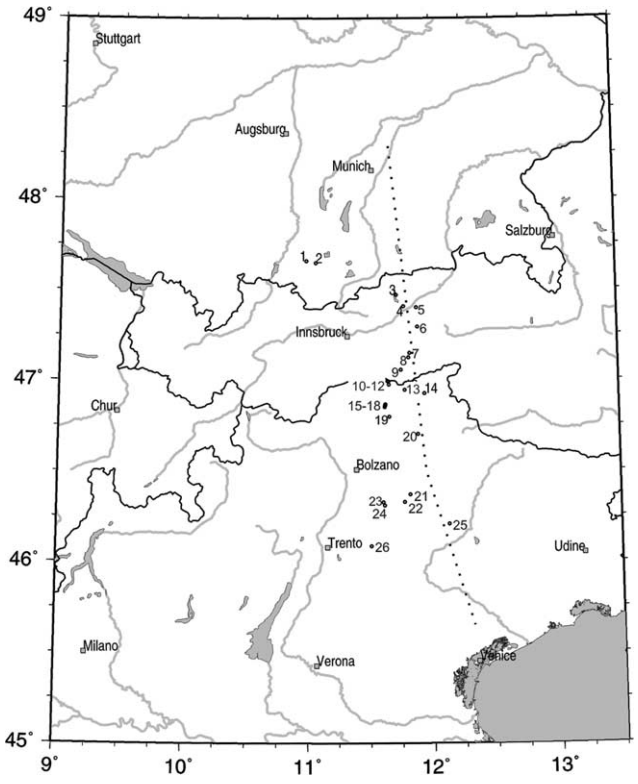

Fig. 1. TRANSALP profile (dotted line) and sampling locations 1–26 (from north to south).

Table 1
Rock types and associated geological units

Location no.	Petrography of sample	Geological unit
1	Sandy-clayey limestone (“Rupelton”)	Molasse (sediment cover European plate)
2	Limy sandstone	Molasse (sediment cover European plate)
3	Fine grained dolomite (“main-dolomite”)	Northern calcareous Alps (cover Adriatic Plate)
4	Dolomitic limestone (“Wetterstein limestone”)	Northern calcareous Alps (cover Adriatic Plate)
5	Muscovite–chlorite–schist (“Wildschönauer Schist”)	Basement Adriatic plate
6	Muscovite–chlorite–carbonate–quartz–phyllite	Basement Adriatic plate
7	Impure limestone (“Hochstegen-marble”)	Tauern Window (basement European plate)
8	Microcline–plagioclase–quartz–biotite–muscovite–ortho-gneiss	Tauern Window (basement European plate)
9	Garnet–bearing ortho-amphibolite	Tauern Window (basement European plate)
10	Garnet–biotite–(ortho?)-amphibolite	Tauern Window (basement European plate)
11	Muscovite–biotite–garnet–epidote–ortho-gneiss	Tauern Window (basement European plate)
12	Garnet–biotite–muscovite–graphite–chlorite–schist	Tauern Window (basement European plate)
13	Muscovite–biotite–garnet–plagioclase–potassium–feldspar–ortho-gneiss	Tauern Window (basement European plate)
14	Biotite–muscovite–potassium–feldspar–schist	Basement Adriatic plate
15	Biotite–muscovite–tourmaline–calcite–schist	Oceanic plate-fragment
16	Garnet–amphibole–biotite–para-gneiss	Basement Adriatic plate
17	Garnet–ortho-amphibolite	Basement Adriatic plate
18	Garnet–biotite–potassium–feldspar–plagioclase–(para?)-gneiss	Basement Adriatic plate
19	Monzogranite/granodiorite (“granite of Brixen”)	Basement Adriatic plate
20	Garnet–biotite–sericite–phyllite	Basement Adriatic plate
21	Very pure dolomite (“Schlern-dolomite”)	Dolomites (coverage Adriatic plate)
22	Biotite–dacite (“quartz-porphyry”)	Dolomites (coverage Adriatic plate)
23	Quartz–monzonite	Basement Adriatic plate
24	Red potassium–feldspar–granite	Basement Adriatic plate
25	Biogene dolomite (“main dolomite”)	Dolomites (coverage Adriatic plate)
26	Granodiorite (“Cima d’Asta granite”)	Basement Adriatic plate

$$\phi = \frac{\rho_r - \rho_b}{\rho_r} = \left(\frac{M}{V_r} - \frac{M}{V_b}\right) \Big/ \frac{M}{V_r} = \frac{(V_b - V_r)}{V_b} \quad (1)$$

Porosity varies for the studied sedimentary rock samples from 0.9% (L4, dolomitic limestone, L7 impure limestone) to 5.7% (L1, sandy-clayey limestone) and for magmatic and metamorphic rocks porosity ranges from 1.0% (L6, muscovite–chlorite–carbonate–quartz–phyllite) to 4.7% (L22, biotite–dacite) (see Tables 1 and 2).

2.2. Thermal conductivity at ambient conditions

Thermal conductivity is isotropic, to a good approximation, for many volcanic and plutonic rocks (Clauser, 1988; Clauser and Huenges, 1995). In contrast to this, thermal conductivity of some sedimentary and many metamorphic rocks is strongly anisotropic. The thermal conductivity of rocks in general decreases with temperature, in contrast to some amorphous or fused materials such as obsidian. The latter will not be discussed in this study.

First, thermal conductivity was determined of all rock samples at ambient temperature of 25 °C with a needle probe (Pribnow, 1994; Popov et al., 1999) which was aligned in different directions to determine anisotropy.

To take into account the effects of porosity, thermal conductivity was measured on water-saturated and dry rock samples. Generally it can be assumed that measurements of the wet rock sample yield more realistic results, since the pore volume in situ is usually water-saturated.

Table 2
Bulk density (ρ) and porosity (ϕ) (sd means standard deviation)

Location no.	ρ (kg m^{-3})	sd ρ (kg m^{-3})	ϕ (%)	sd ϕ (%)
1	2590	20	5.7	0.6
2	2620	70	3.6	2.3
3	2810	100	1.4	1.0
4	2700	40	0.9	0.9
5	2670	30	2.6	1.1
6	2790	20	1.0	1.0
7	2710	40	0.9	0.8
8	2660	10	2.0	0.7
9	2910	20	1.1	0.6
10	2870	80	2.2	1.2
11	2610	40	2.5	1.3
12	2720	20	3.8	0.3
13	2700	20	1.2	1.3
14	2610	40	4.6	1.4
15	2680	50	2.1	1.4
16	2680	30	2.5	0.8
17	2950	50	1.4	1.2
18	2710	60	2.0	1.3
19	2620	30	1.1	0.7
20	2740	60	1.1	0.7
21	2790	50	1.9	1.7
22	2560	70	4.7	2.4
23	2830	40	1.6	0.5
24	2540	40	3.1	1.5
25	2770	30	1.7	1.2
26	2740	20	1.9	0.2

All rock samples were cut to obtain two discs (1) parallel to the plane of bedding or schistosity and (2) perpendicular to the plane of bedding or schistosity.

Measurements on disc (1) were carried out both parallel and normal to the optical axis of elongated minerals. On disc (2) thermal conductivity was determined both parallel and normal to the plane of bedding or schistosity of the rock.

Whenever no bedding or schistosity was visible (e.g. very homogeneous sedimentary rocks or plutonic rocks), two discs in orthogonal directions were cut.

For Eastern Alpine rocks maximum values of thermal conductivity were determined parallel to (1) the optical axis of a mineral or (2) bedding, foliation or schistosity. Measurements normal to (1) the optical axis of a mineral or (2) bedding, foliation or schistosity yield minimum values of thermal conductivity.

Thus we can discriminate between (1) mineral-anisotropy depending on the arrangement of mineral particles (lineation) in the rock sample and (2) shape-anisotropy, occurring parallel and perpendicular to the plane of bedding, foliation or schistosity of a rock volume. Mineral-anisotropy is due to an equal growth orientation of minerals in the rock (e.g. elongated and orientated amphiboles). Shape-anisotropy is due to a change of material (e.g. alternating quartz- and feldspar- or mica-layers) inside a sedimentary or metamorphic rock.

The anisotropy factor (af) is defined by the ratio of parallel and normal components of thermal conductivity (Cermak and Rybach, 1982).

$$\mathrm{af}_{\mathrm{mineral}} = \frac{\lambda_{\mathrm{par(lineation)}}}{\lambda_{\mathrm{norm(lination)}}}; \quad \mathrm{af}_{\mathrm{shape}} = \frac{\lambda_{\mathrm{par(foliation)}}}{\lambda_{\mathrm{norm(foliation)}}} \qquad (2)$$

The variance of values, average values and anisotropy factors of thermal conductivity was determined and calculated both for lineation (Fig. 2a) and foliation (Fig. 2b).

In absence of visible layering or foliation the anisotropy factor of thermal conductivity was calculated from the ratio of the higher and lower average value of thermal conductivity.

A sample is isotropic when it has an anisotropy factor of 1. Anisotropy factors lower than 0.9 or higher than 1.1 indicate a bedding, foliation or lineation with a significant effect on thermal conductivity. The highest anisotropy factor of approximately 1.6 (Fig. 2b) was asserted for the garnet–biotite–muscovite–graphite–chlorite–schist from the Tauern Window (L12) while especially effusive and intrusive magmatic rocks of the Adriatic basement (L22, L23, L24, L26) show nearly isotropic thermal conductivity properties.

The highest thermal conductivity values of around 6 $\mathrm{W\,m^{-1}\,K^{-1}}$ were determined for dolomites from the locations L3 and L21 (Table 1). The high thermal conductivity values for dolomites from the Eastern Alps

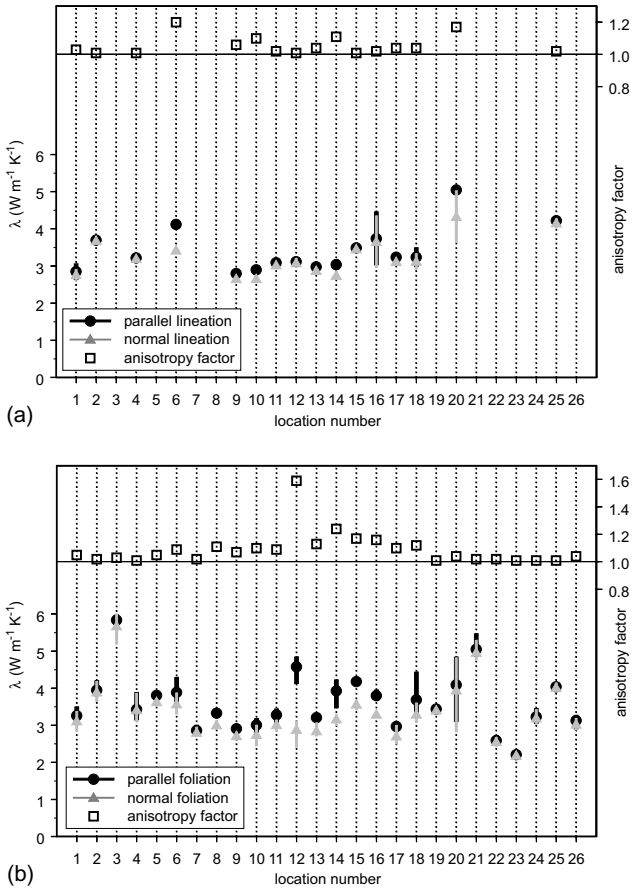

Fig. 2. Scattering of laboratory measurements of the thermal conductivity (vertical bars), mean values (symbols) and anisotropy factors (squares) of 26 suits of water saturated rocks at ambient conditions (25 °C): plane of measurement (a) parallel and normal to lineation; (b) parallel and normal to bedding, foliation or schistosity of the rock.

corresponds nicely with literature data (see also Clauser and Huenges, 1995).

High anisotropy of thermal conductivity of rocks with visible foliation (metamorphic rocks) can probably be interpreted as an alternation of strong and weak-conductive layers (e.g. quartz—or feldspar—respective mica-layers) or a high content of oriented minerals with strong anisotropy (e.g. mica).

2.3. Temperature dependence of thermal conductivity

The temperature dependence of thermal conductivity was studied on dry samples for temperatures ranging from 0 to 500 °C using a divided bar device. Due to the increased inter-granular contact resistance within the dry rock samples, thermal conductivity at ambient conditions for these measurements is usually lower than that determined by the needle probe on the water-saturated rocks. Fig. 3a and b shows the coupled effect of mineralogical composition and temperature for magmatic rocks (L9, L19, L22, L23; see Table 1), meta-

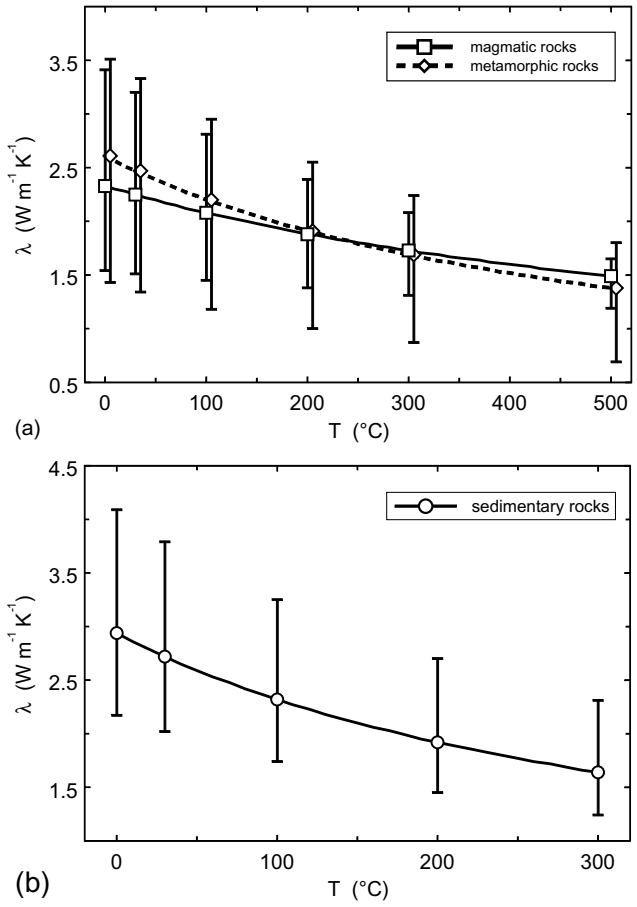

Fig. 3. Mean values (symbols) and ranges of variation (vertical bars) of thermal conductivity λ with temperature for (a) magmatic and metamorphic and (b) sedimentary rocks.

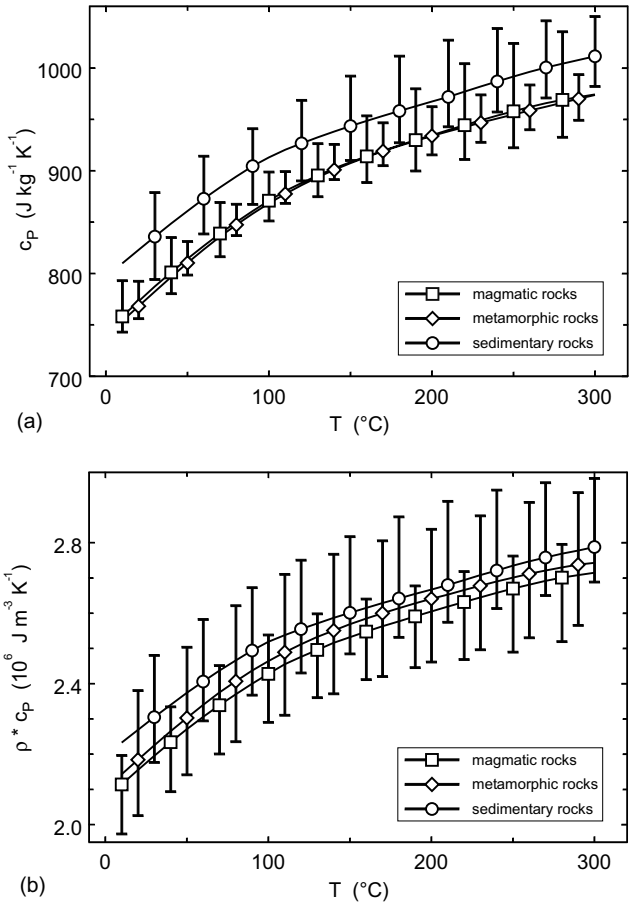

Fig. 4. Mean values and ranges of variation of (a) specific heat capacity c_p at constant pressure and (b) thermal capacity ($\rho \times c_p$) as a function of temperature of for magmatic, metamorphic, and sedimentary rocks. The sampling rate of the device is $\Delta T = 0.05$ K. For better visualization mean values of data points (symbols) as well as minimum and maximum value (bars) are displayed in an interval of 30 K.

morphic rocks (L6, L10, L11, L12, L14, L16, L17) and sedimentary rocks (L1, L2, L4, L5, L21). For rocks with a large thermal conductivity at ambient conditions (λ_{rt}) the decrease in thermal conductivity with temperature is more pronounced than for rocks with a low λ_{rt}. As anisotropy of the rock matrix usually decreases with increasing temperature (Seipold, 2001), it becomes negligible at high temperatures. Therefore it was not considered in our study.

2.4. Temperature dependence of thermal capacity

The thermal capacity is the product of density ρ and specific heat capacity c_p. Specific heat capacity c_p at constant pressure was determined as a function of temperature for at least one rock sample from each rock unit using a dynamic differential heat flow calorimeter from ambient temperatures to 300 °C, the maximum temperature range of the device. Fig. 4a shows the mean values of these measurements for magmatic, metamorphic, and sedimentary rocks (same rock samples as Fig. 3a and b; Table 1). Specific heat capacity measured at ambient conditions ranges from 740 to 850 $J\,kg^{-1}\,K^{-1}$ and is highest in sedimentary rocks. It increases with temperature to maximum values of around 1050 $J\,kg^{-1}\,K^{-1}$ (Fig. 4a). Since the thermal cubic expansion coefficient is very small for rocks, the density was regarded as constant over the temperature range of 1–300 °C. The specific heat capacity c_p and the thermal capacity ($\rho \times c_p$) as a function of temperature (Fig. 4a and b) differ by a constant factor only—the density ρ—which depends solely on the sample (rock composition). It increases with temperature from around 2×10^6 $J\,m^{-3}\,K^{-1}$ at ambient temperature to maximum values of 3×10^6 $J\,m^{-3}\,K^{-1}$ (Fig. 4b) at a temperature of 300 °C.

2.5. Temperature dependence of thermal diffusivity

The thermal diffusivity describes the equilibration of a temperature imbalance. It is a function of thermal conductivity λ, density ρ and specific heat capacity c_p at a constant pressure:

$$\kappa = \frac{\lambda}{\rho \times c_p} \tag{3}$$

Fig. 5a shows the values of thermal diffusivity in the temperature range of 1–300 °C.

The thermal conductivity decreases with temperature (Fig. 3a and b) while the specific heat capacity (Fig. 4a) increases with temperature. Since in Eq. (3) thermal conductivity is in the numerator and specific heat capacity in the denominator, thermal diffusivity decreases more than thermal conductivity with temperature (Fig. 5a). The thermal conductivity decreases between 25% and 44% in the temperature interval 1–300 °C, the thermal diffusivity however by 42–54%.

In Fig. 5b thermal diffusivity at ambient temperature is plotted versus thermal conductivity. A linear regression yields a slope (see function 3) of $1/(\rho \times c_p) = 1/(2.2 \times 10^6\ \mathrm{J\,m^{-3}\,K^{-1}})$. This agrees with Beck's (1988) result $(\rho \times c_p) = (2.3 \times 10^6\ \mathrm{J\,m^{-3}\,K^{-1}}) \pm 20\%$.

3. Developing a general equation for $\lambda(T)$

In the following, we use an approach similar to Sass et al. (1992) to obtain values for thermal conductivity for different crystalline rocks from the Eastern Alps. Based on the results for metamorphic rocks (gneisses, amphibolites and phyllites: L6, L10, L11, L14, L16, L17) and magmatic rocks (L9, L19, L22, L23) we plot the normalized thermal resistivity $\lambda(0)/\lambda(T)$ versus temperature (Fig. 6a). Linear regression yields slopes and intercepts for all rocks studied. The average intercept of 0.99 yield an error of ±1%. From linear regression of the slope versus thermal resistivity $1/\lambda(0)$ we then obtained the coefficients for crystalline rock samples (Fig. 6b). The resulting equation for $\lambda(T)$ for magmatic and metamorphic rocks is:

$$\lambda(0) = 0.53\lambda(25) + \frac{1}{2}\sqrt{1.13(\lambda(25))^2 - 0.42\lambda(25)} \tag{4}$$

$$\lambda(T) = \frac{\lambda(0)}{0.99 + T(a - b/\lambda(0))} \tag{5}$$

with $a = 0.0030 \pm 0.0015$ and $b = 0.0042 \pm 0.0006$.

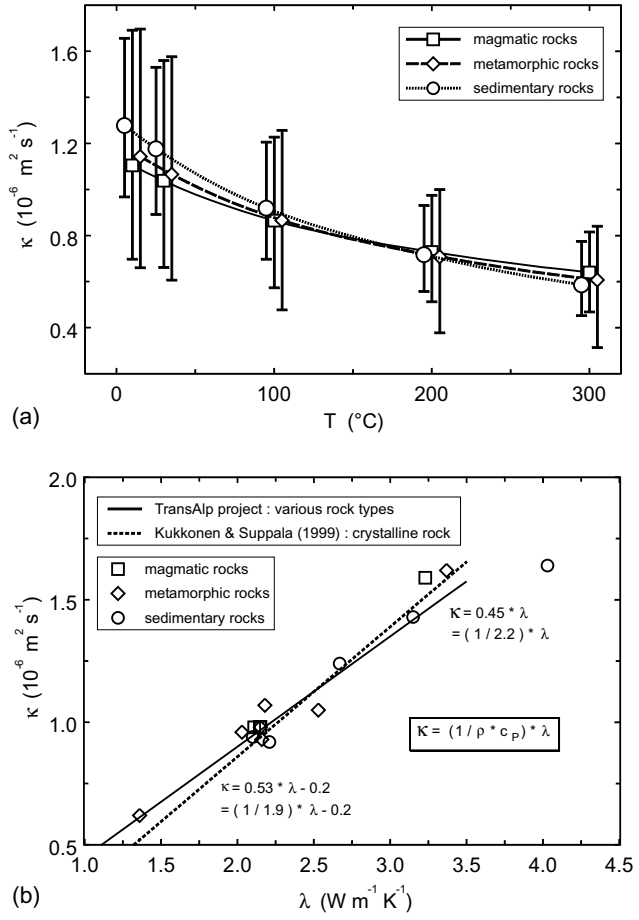

Fig. 5. (a) Mean values (symbols) and ranges of variation (vertical bars) of thermal diffusivity as a function of temperature and (b) thermal diffusivity as a function of thermal conductivity for magmatic, metamorphic, and sedimentary rocks.

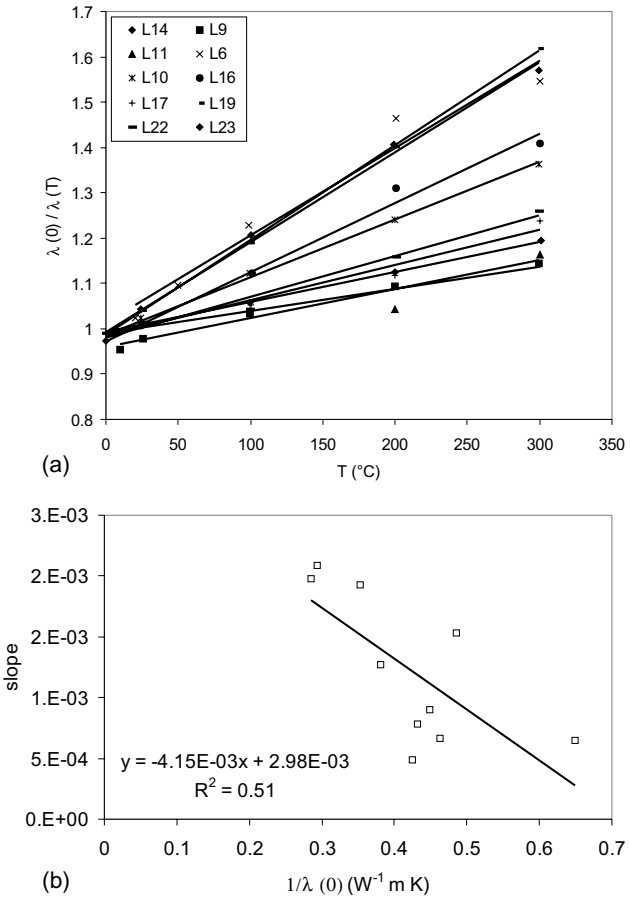

Fig. 6. Determination of coefficients of $\lambda(T)$ for different crystalline rocks of the Eastern Alps: (a) normalized thermal resistivity $\lambda(0)/\lambda(T)$ versus temperature; (b) slope of (a) versus $1/\lambda(0)$.

The TRANSALP data set (L1, L2, L4, L5, L21) and supplementary data from measurements of 23 limestones, dolomites and sandstones from the Molasse Basin (Clauser et al., 2002) were used to determine coefficients for a general equation for $\lambda(T)$ for sedimentary rocks as well. A first metamorphosis of sedimentary rocks occurs at temperatures of around 300–350 °C (matching a depth level of 10–12 km). Thus we verified the equation for temperatures from 0 to 300 °C. The equation for $\lambda(T)$ of sedimentary rocks was determined in the same way (as described above) and can be formulated as:

$$\lambda(0) = 0.54\lambda(25) + \frac{1}{2}\sqrt{1.16(\lambda(25))^2 - 0.39\lambda(25)} \quad (6)$$

$$\lambda(T) = \frac{\lambda(0)}{0.99 + T(a - b/\lambda(0))} \quad (7)$$

with $a = 0.0034 \pm 0.0006$ and $b = 0.0039 \pm 0.0014$.

Above 500–600 °C a linear fit of $(1/\lambda)$ is no longer permissible because of the increasing importance of heat transfer by radiation (Clauser and Huenges, 1995). Therefore, we studied the temperature dependence of thermal conductivity for crystalline rocks in the temperature range of 0–500 °C. The coefficients of Sass et al. (1992) for different crystalline rocks from the TRANSALP data set yield good results for temperatures up to 300 °C but show systematic differences for temperatures above 300 °C (Fig. 7a). Applying Eq. (5) to the TRANSALP data set shows a maximum error of 15% for the temperature range 300–500 °C.

For different sedimentary rocks the corresponding comparison of thermal conductivity calculated with the coefficients of Sass et al. (1992) and measured values shows a deviation of approximately 10% for temperatures below 80 °C (Fig. 7b). For higher temperatures, the deviation between calculated and measured values rises systematically. Therefore the coefficients for crystalline rocks of Sass et al. (1992) can no longer be used for sedimentary rocks. The coefficients of this study (Eq. (7)) yield a maximum error of +8/−34% in the temperature range 150–300 °C (Fig. 7b).

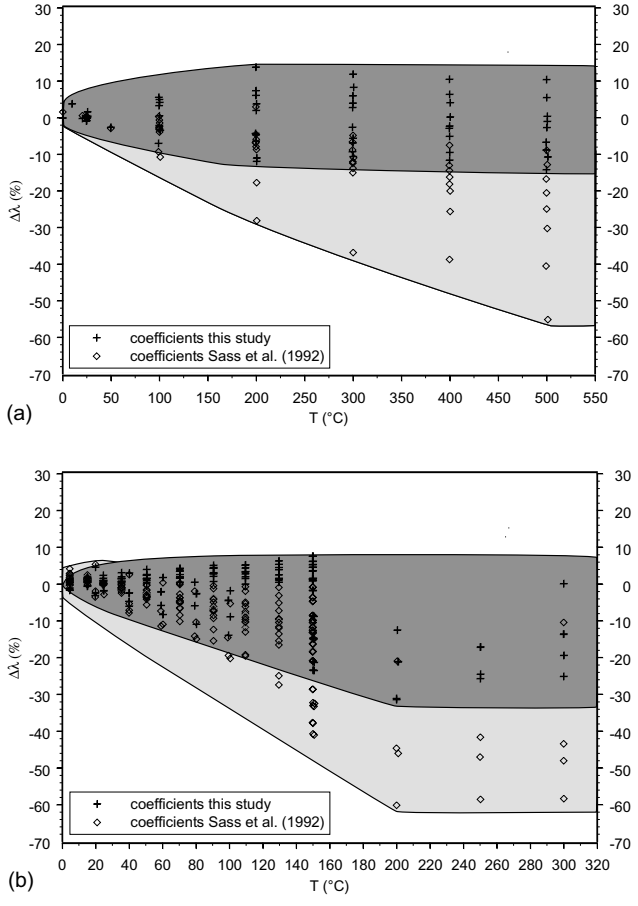

Fig. 7. Deviation of λ (measured) and λ (calculated) versus temperature for different crystalline and sedimentary rocks (ordinate: λ (measured) – λ (calculated) in percent). Open diamonds: calculated with the coefficients of Sass et al. (1992); black crosses calculated with coefficients of this study (shading): (a) crystalline rocks; (b) sedimentary rocks.

4. Comparison with other expressions for thermal conductivity

A frequently used general empirical equation for the temperature dependence of thermal conductivity was given by Zoth and Hänel (1988). They postulated the temperature dependence of thermal conductivity $\lambda(T)$ to be:

$$\lambda(T) = \frac{A}{(350 + T)} + B \quad (8)$$

where A and B are coefficients which depend on the type of rock (λ in $\mathrm{W\,m^{-1}\,K^{-1}}$, T in °C).

Based on measurement on different rock types in the range 0–800 °C they calibrated the empirical equations:

$$\lambda(T) = \frac{705}{(350 + T)} + 0.75 \quad (9)$$

for metamorphic rocks (e.g. amphibolite, phyllite);

$$\lambda(T) = \frac{807}{(350 + T)} + 0.64 \quad (10)$$

for acid rocks (e.g. granite, granodiorite, quartz porphyry);

$$\lambda(T) = \frac{474}{(350 + T)} + 1.18 \quad (11)$$

for basic rocks (basalt, gabbro);

$$\lambda(T) = \frac{1293}{(350 + T)} + 0.73 \quad (12)$$

for ultrabasic rocks (dunite, olivinite, peridotite);

$$\lambda(T) = \frac{1073}{(350 + T)} + 0.13 \tag{13}$$

for limestone.

Excluding salt and ultrabasic rocks, they summarized the average temperature dependence of thermal conductivity for different rocks as:

$$\lambda(T) = \frac{770}{B(350 + T)} + 0.7 \tag{14}$$

Comparing Eq. (5) with the equations of Zoth and Hänel (1988) we can see that for different types of rock—including ultrabasic rocks the equation of this study yields nearly the same results as the respective equations of Zoth and Haenel (Fig. 8a and b). This also confirms that our approach of using a suite of both magmatic and metamorphic rocks from different crustal levels from the Eastern Alps yields a good estimate for a general equation of $\lambda(T)$ for crystalline rocks.

However, Eq. (7) cannot be applied to determine $\lambda(T)$ for salt rocks due to the higher temperature dependence of salt compared to other sedimentary rocks (Fig. 8b).

The comparison of Eq. (5) and that of Sass et al. (1992) shows slight differences especially for acid, basic and metamorphic rocks (Fig. 8c). Similar to the different equations of Zoth and Haenel, Eq. (5) shows a stronger decrease of thermal conductivity with temperature above 200 °C.

Seipold (1998, 2001) used different expressions for the temperature dependence of thermal conductivity. He used a large number of measurements and additional literature data to determine a linear decrease of $\lambda(T)$. A temperature function can thus be written as:

$$\lambda(T) = \frac{1}{B(T - 532 \pm 45)} + 0.448 \pm 0.014 \tag{15}$$

with a linear correlation coefficient of $R = -0.84$.

B is a coefficient which depends on rock type and T, is temperature in K. The linear fit of $\lambda(T)$ shows a slight variation of around 0.5 W/m K compared to the results of Eq. (5) (Fig. 9a).

For many rocks Seipold obtained a better fit of the data with the equation:

$$\lambda(T) = \frac{T}{F(T - 314 \pm 35)} + 122 \pm 20 \tag{16}$$

with a linear correlation coefficient $R = -0.75$.

For temperatures above 600 °C Seipold implemented an additional cubic term $C' \times T^3$ to take into account the contributions of electromagnetic radiation. The respective expression can be written as:

$$\lambda(T) = \frac{1}{(A' + B' \times T)} + C' \times T^3 \tag{17}$$

with different coefficients A', B' and C' for different types of rock. The comparison of Eqs. (5) and (17) (Fig. 9b) shows that above 100 °C the curves for rocks with either very large or very low thermal conductivity at ambient conditions differ significantly. The fit of Seipold for these rocks leads to a smaller decrease in thermal conductivity with temperature than ours. As Seipold (2001) specifies the standard deviation of the fit of all curves to the measured data to be ± 0.3 W m^{-1} K^{-1}, the deviation to our curve would most certainly be lower if the measured data were grouped according to the procedure in this study.

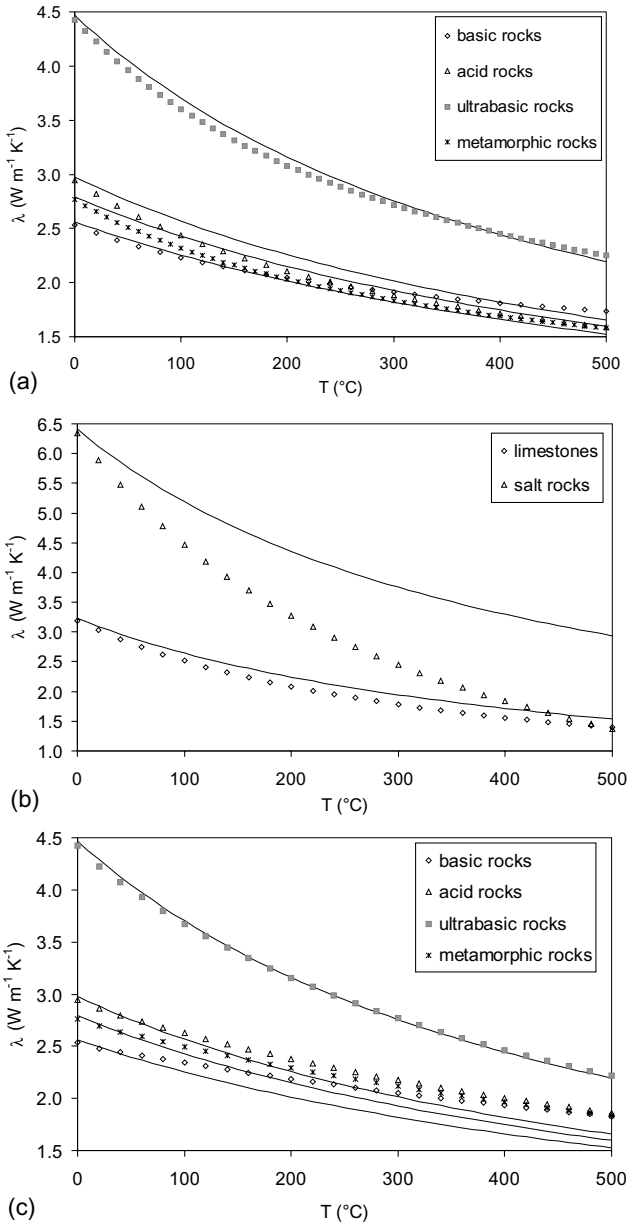

Fig. 8. Comparison of the equations of this study with different general equations for $\lambda(T)$. Lines correspond to Eqs. (5) and (7) and symbols to: (a) Zoth and Hänel (1988) different crystalline rocks; (b) Zoth and Hänel (1988) sedimentary rocks, (c) Sass et al. (1992) different crystalline rocks.

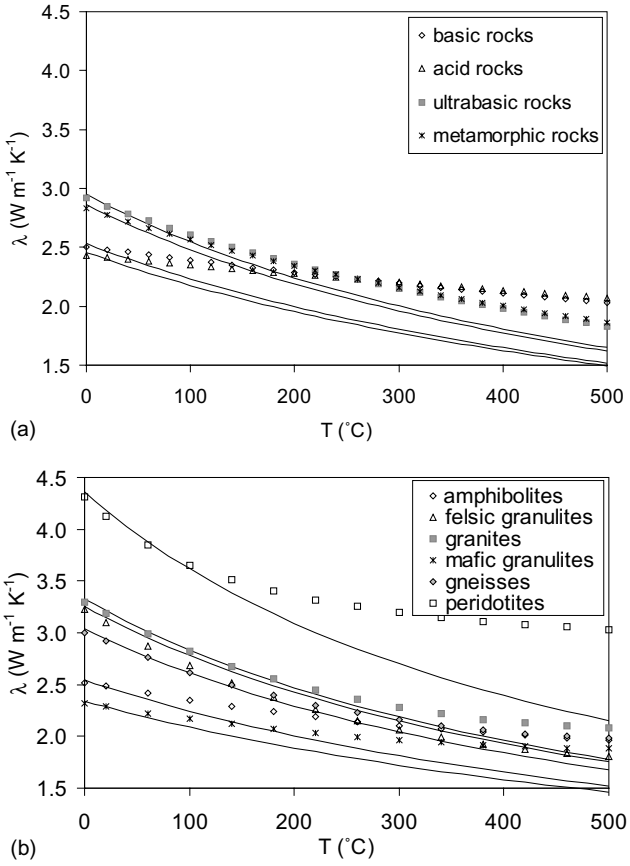

Fig. 9. Comparison of Eq. (5) for crystalline rocks of this study with $\lambda(T)$ according to Seipold (1998). Lines are results from Eq. (5), symbols are results from Seipold (1998) and Seipold (2001): (a) Eq. (15); (b) Eq. (17).

5. Conclusions

We find that the thermal conductivity at 0 °C characterizes the temperature dependence of thermal conductivity for different types of rock. There is no substantially different behavior for different rock types. This is also observed for different sedimentary rocks. Because genesis and mineralogical composition of these two rock-categories are fundamentally different, two separate sets of coefficients are necessary. We verified the equation of Sass et al. (1992) using the TRANSALP data—and show that the original coefficients of Sass et al. (1992) can be used to estimate the temperature dependence of thermal conductivity for crystalline rocks up to 300 °C. Above 300 °C the coefficients of Sass et al. (1992) yield an error that increases with temperature. Using the coefficients of Sass et al. to determine $\lambda(T)$ for sedimentary rocks also yields errors. For temperatures above 300 °C, the coefficients of this study for $\lambda(T)$ of crystalline rocks yield an improved fit to the data set from the Eastern Alps. The corresponding equation for $\lambda(T)$ for different types of sedimentary rock also fits the data better than that of Sass et al. (1992) and yields fits comparable to that of Zoth and Hänel (1988).

Acknowledgements

We are grateful to N. Klitzsch for many helpful suggestions and comments and to L. Rybach and an anonymous reviewer for thoughtful reviews. C. Clauser and H. Trautmann helped us a lot to improve the manuscript. Special thanks to H.-W. Fesche (Leibniz Institute for Applied Geosciences, Hannover) who helped us to cope with fatigue of material of high temperature components of the divided bar. We also want to thank K.P. Burgath and M. Mohr (Federal Institute of Geosciences and Natural Resources (BGR), Hannover) for carrying out extensive thin section microscopy and X-ray fluorescence in order to provide a proper rock naming. D. Behain helped us by carrying out density measurements, using facilities advised by H.-G. Dietrich (Federal Institute of Geosciences and Natural Resources (BGR), Hannover). The German Science Foundation supported this project under grant number CL 141/10-(1, 2) to C. Clauser and B. Lammerer.

Appendix A. Measurement techniques

The rock volume was determined with a gas displacement pycnometer. This instrument measures the volume of solid objects of irregular shape, whether powdered or coherent. The gas displacement pycnometer consists of a calibrated and helium-filled sample chamber and an expansion chamber, both connected by a valve. The chamber containing the sample is then filled with helium up to a high pressure. When the closed valve is opened, the pressure will drop to an intermediate value. The rock volume of the sample is then determined by measuring the change in pressure and temperature of the calibrated volume of both chambers, using the mass balance equation. The device then uses the rock volume and the weight of the sample to calculate the rock density. To calculate the bulk density of a rock sample, a quantity of a free-flowing dry medium (e.g. ''DryFlo'') is placed in a sample chamber and its volume is measured. A rock sample is then placed in the chamber with the medium, and the volume is measured again. Because the free-flowing dry medium does not enter the rock's pores, the difference between the two measurements is the displacement volume of the sample including its pores. The envelope volume and the weight of the rock sample are then used to calculate its ''envelope'' or bulk density.

We measured thermal conductivity at an ambient temperature of approximately 25 °C on all rock samples

(water saturated and dry) with a needle probe (Pribnow, 1994; Popov et al., 1999). This method was chosen primarily because of its easy use and simple sample preparation. In addition, thermal conductivity was determined up to 500 °C using a divided bar device. This technique is highly specific and time consuming, in particular at elevated temperatures. Sample preparation can be difficult and problems were encountered with a couple of samples. Therefore, these measurements were performed on a selected set of rock samples, representing the main rock units.

There are two major differences between needle probe measurements and the divided bar (Pribnow et al., 2000, appendix): (1) the needle probe method is a transient while the divided-bar is steady-state; (2) the divided-bar measurements yield thermal conductivity in the direction parallel to the divided-bar axis, whereas the needle probe method yield thermal conductivity in a plane perpendicular to the needle probe axis.

The needle probe is based on the theory of a line source in an infinite medium (Carslaw and Jaeger, 1947, section 10.4). In practice, it is a needle probe embedded in and flush with the surface of a material of very low thermal conductivity (Pribnow and Sass, 1995). This device is known as half-space line source. It is a portable advanced development of the version used in the field laboratory at the super-deep drill hole (KTB) in Germany. Data analysis is described in detail by Huenges et al. (1990). The needle probe consists of a cylindrical probe of 2 mm in diameter and 70 mm in length. A thermometer at the centre of the needle probe records the probe temperature. According to Kappelmeyer and Haenel (1974, section 4.1), the probe length can be assumed to be infinite. The needle probe is embedded in a cylindrical block of transparent plastic such as ''Plexiglass'' or ''Perspex''. The heat propagation into the sample is approximately 6–12 mm (Honarmand, 1993) depending on the thermal conductivity of the material. This was taken into account selecting and preparing the sample. Needle probe measurements return a scalar value of thermal conductivity from a plane perpendicular to the needle probe axis. For anisotropic material it is theoretically possible to obtain the principal values of the thermal conductivity tensor. Theory, practical experiences and uncertainty of such measurements are discussed in detail in Grubbe et al. (1983) and Popov et al. (1999).

The divided-bar (Beck, 1988) is a steady state comparative method to determine thermal conductivity of solid rock samples or a cylindrical cell (Sass et al., 1971) containing water-saturated material, which may be loose. The latter technique is only viable at low temperatures (0–60 °C) (Pribnow et al., 2000, appendix).

The basic concept of this method is to compare the unknown thermal conductivity of a rock sample to the known thermal conductivity of reference material. The sample and reference materials are shaped into discs with a diameter of 50 mm and approximately the same thickness (10 mm). The reference material is pyroceram, which has a conductivity comparable to that of rock samples. The heat flows parallel to the divided-bar axis (stack) from a heater A (high temperature level) to a second heater B (low temperature level) through two reference disks and the sandwiched rock sample. The radial heat flow can be neglected because guard heaters and insulating material minimize it. A thermal compound is used to reduce the contact resistance between the reference and the rock samples. The temperature drop across the rock sample is compared to that across the reference sample of known thermal conductivity. Assuming the heat flow through the system (stack) to be constant, the unknown thermal conductivity of the rock sample can be calculated.

The specific heat capacity is a scalar value and an isotropic physical property; it increases with temperature for solid rock material. A heat flux differential scanning calorimeter (Heat Flux DSC) was used to determine the specific heat capacity of rock samples as a function of temperature up to 300 °C, the maximum temperature range of the used device.

Our Heat Flux DSC consists of a block-type cylindrical furnace with two cylindrical cavities (Hemminger and Cammenga, 1989; Höhne et al., 1996), holding the sample and reference containers, which are connected to the furnace with several thermocouples (thermopile). These containers (measuring systems) are thermally decoupled (Calvet, 1948) with a programmable temperature controller. The characteristic feature of the used device is the symmetrical (twin-type) design and the system measuring only the difference in temperature between the two containers (with thermopiles instrumented containers) (Hemminger and Cammenga, 1989; Höhne et al., 1996). When the furnace is heated, generally linearly in time, heat flows between the furnace and the sample container including a sample as well as between the furnace and the empty reference container. The heat flow rates are proportional to the measured temperatures at the thermopiles. The interesting differential signal, a small change in the heat flow rate, is affected by the change of the specific heat capacity of rock samples. The decisive advantage of the differential principle is that disturbances, such as temperature variations in the environment of the measuring system, affect the two measuring systems equally and are compensated when the difference between the individual signals is formed (Höhne et al., 1996). Hemminger and Cammenga (1989) and Höhne et al. (1996) offer a detailed description of the used Heat Flux DSC instrument, a comparison to other devices, and the theory of DSC systems.

References

Beck, A.E., 1988. Methods for determining thermal conductivity and thermal diffusivity. In: Haenel, R., Rybach, L., Stegena, L. (Eds.), Handbook of Terrestrial Heat-Flow Density Determination. Kluwer Academic Publishers, Dordrecht.

Birch, F., Clark, H., 1940. The thermal conductivity of rocks and ist dependence upon temperature and composition. Am. J. Sci. 238, 613–635.

Calvet, E., 1948. C.R. Hebd. Acad. Sci. 226, 1702–1704.

Carslaw, H., Jaeger, J.C., 1947. Conduction of Heat in Solids. Clarendon, Oxford.

Cermak, V., Rybach, L., 1982. Thermal conductivity and specific heat of minerals and rocks. In: Landolt-Börnstein: Numerical Data and Functional Relationships in Science and Technology. Group V (Geophysics and Space Research), Berlin-Heidelberg, Springer.

Clauser, C., 1988. Opacity—the concept of radiative thermal conductivity. In: Haenel, R., Rybach, L., Stegena, L. (Eds.), Handbook of Terrestrial Heat-Flow Density Determination. Kluwer Academic Publishers, Dordrecht.

Clauser, C., Huenges, E., 1995. Thermal conductivity of rocks and minerals. In: AGU Reference Shelf 3 Rock Physics and Phase Relations. A Handbook of Physical Constants. pp. 105–125.

Clauser, C., Deetjen, H., Höhne, F., Rühaak, W., Hartmann, A., Schellschmidt, R., Rath, V., Zschocke, A., 2002. Erkennen und Quantifizieren von Strömung: Eine geothermische Rasteranalyse zur Klassifizierung des tiefen Untergrundes in Deutschland hinsichtlich seiner Eignung zur Endlagerung radioaktiver Stoffe, Endbericht zum Auftrag 9X0009-8390-0 des Bundesamtes für Strahlenschutz (BfS). Angewandte Geophysik, RWTH Aachen, 159 pp.

Grubbe, K., Haenel, R., Zoth, G., 1983. Determination of the vertical component of thermal conductivity by line source methods. Zeitschrift für Geologie und Paläontologie, Teil I H (1/2), pp. 49–56.

Hemminger, W.F., Cammenga, H.K., 1989. Methoden der Thermischen Analyse. Springer-Verlag, Berlin, Heidelberg, New York.

Höhne, G., Hemminger, W., Flammersheimer, H.-J., 1996. Differential Scanning Calorimety—An Introduction for Practioners. Springer-Verlag, Berlin, Heidelberg, New York.

Honarmand, H., 1993. Bohrlochsonden zur Bestimmung der Wärmeleitfähigkeit in größeren Tiefen. Verlag für Wissenschaft und Forschung, Berlin.

Huenges, E., Burkhardt, H., Erbas, K., 1990. Thermal conductivity profile of the KTB pilot corehole. Scientific Drill. 1, 224–230.

Kappelmeyer, O., Haenel, R., 1974. Geothermics. Gebrüder Bornträger, Berlin, Stuttgart.

Popov, Y.A., Pribnow, D., Sass, J.H., Williams, C.F., Burkhardt, H., 1999. Characterization of rock thermal conductivity by high-resolution optical scanning. Geothermics 28 (2), 253–276.

Pribnow, D.F.C., 1994. Ein Vergleich von Bestimmungsmethoden der Wärmeleitfähigkeit unter Berücksichtigung von Gesteinsgefügen und Anisotropien. VDI-Verlag GmbH, Düsseldorf.

Pribnow, D.F.C., Sass, J.H., 1995. Determination of thermal conductivity for deep boreholes. J. Geophys. Res. 100 (B6), 9981–9994.

Pribnow, D.F.C., Davis, E.E., Fisher, A.T., 2000. Borehole heat flow along the eastern flank of the Juan de Fuca Ridge, including effects of anisotropy and temperature dependence of sediment thermal conductivity. J. Geophys. Res. 105 (13), 13,449–13,456.

Pribnow, D.F.C., Davis, E.E., Fisher, A.T., 2000. Borehole heat flow along the eastern flank of the Juan de Fuca Ridge, including effects of anisotropy and temperature dependence of sediment thermal conductivity. J. Geophys. Res. 105 (Appendix).

Sass, J.H., Lachenbruch, A.H., Munroe, J., 1971. Thermal conductivity of rocks from measurements on fragments and its application to heat-flow determination. J. Geophys. Res. 76, 3391–3401.

Sass, J.H., Lachenbruch, A.H., Moses, T., Morgan, P., 1992. Heat flow from a scientific research well at Cajon Pass, California. J. Geophys. Res. 97, 5017–5030.

Seipold, U., 1998. Temperature dependence of thermal transport properties of crystalline rocks—a general law. Tectonophysics 291, 161–171.

Seipold, U., 2001. Der Wärmetransport in kristallinen Gesteinen unter den Bedingungen der kontinentalen Kruste. Scientific Technical Report STR01/13, Geoforschungszentrum (GFZ), Potsdam.

Sibbitt, W.L., Dodson, J.G., Tester, J.W., 1979. Thermal conductivity of crystalline rocks associated with energy extraction from hot dry rock geothermal systems. J. Geophys. Res. 84, 1117–1124.

TRANSALP Working Group, 2002. First deep seismic reflection images of the Eastern Alps reveal giant crustal wedges and transcrustal ramps. Geophys. Res. Lett. 29 (10), 92-1–92-3.

Zoth, G., Hänel, R., 1988. Appendix. In: Haenel, R., Rybach, L., Stegena, L. (Eds.), Handbook of Terrestrial Heat-Flow Density Determination. Kluwer Academic Publishers, Dordrecht.